

Linking bacterial population dynamics and nutrient removal in the granular sludge biofilm ecosystem engineered for wastewater treatment

David G. Weissbrodt, Noam Shani & Christof Holliger

Laboratory for Environmental Biotechnology, School of Architecture, Civil and Environmental Engineering, Institute of Environmental Engineering, Ecole Polytechnique Fédérale de Lausanne, Lausanne, Switzerland

Correspondence: David Weissbrodt, EPFL ENAC IIE LBE, Station 6, CH-1015 Lausanne, Switzerland. Tel.: +41 21 693 6192/+41 58 765 5028; fax: +41 21 693 4722; e-mails: david.weissbrodt@epfl.ch and david.weissbrodt@ifu.baug.ethz.ch

Present addresses: David G. Weissbrodt, Chair of Process Engineering in Urban Water Management, Institute of Environmental Engineering, ETH Zürich, Zürich, Switzerland, and Department of Process Engineering, Eawag – Swiss Federal Institute of Aquatic Science and Technology, Dübendorf, Switzerland

Present address: Noam Shani, Agroscope, Institute for Food Sciences, Bern, Switzerland

Received 21 October 2013; revised 7 March 2014; accepted 8 March 2014. Final version published online 14 April 2014.

DOI: 10.1111/1574-6941.12326

Editor: Alfons Stams

Keywords

biological wastewater treatment; aerobic granular sludge; bacterial community structure; PyroTRF-ID methodology; multivariate numerical analyses.

Introduction

When compared to conventional wastewater treatment systems based on activated sludge flocs, sequencing batch reactors (SBR) using aerobic granular sludge (AGS) biofilms have the advantage to achieve simultaneous biological nutrient removal (BNR) at high conversion rates and with low impact on land area. In both types of systems, efficient management of the underlying bacterial resource and understanding of the impact of fluctuations in opera-

Abstract

Intensive nutrient removal from wastewater in anaerobic–aerobic systems using granular sludge should rely on optimal balances at biofilm and microbial ecology levels. This study targets the impacts of reactor characteristics and fluctuations in operation conditions on nutrient removal and bacterial community structures by means of microbial and numerical ecology methods. The dynamics of both predominant and accompanying populations were investigated with high resolution on temporal and phylogenetic scales in two reactors operated during 5 months with synthetic wastewater. Multivariate analyses highlighted significant correlations from process to microbial scales in the first reactor, whereas nitrification and phosphorus removal might have been affected by oxygen mass transfer limitations with no impact at population level in the second system. The bacterial community continuum of the first reactor was composed of two major antagonistic *Accumulibacter-Nitrosomonas-Nitrospira* and *Competibacter-Cytophaga-Intrasporangiaceae* clusters that prevailed under conditions leading to efficient P- (> 95%) and N-removal (> 65%) and altered P- (< 90%) and N-removal (< 60%), respectively. A third cluster independent of performances was dominated by *Xanthomonadaceae* affiliates that were on average more abundant at 25 °C (31 ± 5%) than at 20 °C (22 ± 4%). Starting from the physiological traits of the numerous phylotypes identified, a conceptual model is proposed as a base for functional analysis in the granular sludge microbiome and for future investigations with complex real wastewater.

tion conditions at community level is required for robust performances.

In activated sludge and granular sludge ecosystems, BNR is subjected to the competition between polyphosphate- (PAO) and glycogen-accumulating organisms (GAO) that are most often related to ‘*Candidatus* *Accumulibacter phosphatis*’ and ‘*C. Competibacter phosphatis*’ (hereafter referred to as *Accumulibacter* and *Competibacter*), respectively (Hesselmann *et al.*, 1999; Crocetti *et al.*, 2002; de Kreuk & van Loosdrecht, 2004; Oehmen *et al.*, 2007;

Lemaire *et al.*, 2008; Lopez-Vazquez *et al.*, 2009b; Ebrahimi *et al.*, 2010; Gonzalez-Gil & Holliger, 2011; Weissbrodt *et al.*, 2013a, b). Bacterial selection mechanisms are triggered by specific operation and microenvironmental conditions, with pH, temperature, carbon sources, nutrient ratios, and sludge retention time (SRT) as key factors (Oehmen *et al.*, 2010a; Winkler *et al.*, 2011; Weissbrodt *et al.*, 2013b).

The denitrifying metabolic properties of certain clades of *Accumulibacter* and *Competibacter* have been used to implement simultaneous BNR in AGS by selecting for different bacterial niches along gradients of dissolved nutrients and oxygen (DO) inside granules (Kishida *et al.*, 2006; de Kreuk *et al.*, 2007; Lemaire *et al.*, 2008; Yilmaz *et al.*, 2008; Lochmatter *et al.*, 2013). However, these studies have not converged towards a uniform conclusion on the involvement of either PAO or GAO in denitrification, and it has been recently suggested that denitrification in anaerobic-aerobic AGS reactors might not be restricted to only PAO and GAO (Weissbrodt *et al.*, 2013a). At the actual state of knowledge, an adequate balance of these organisms should be maintained in AGS for efficient BNR, such as $48 \pm 18\%$ of PAO and $26 \pm 8\%$ of GAO forming a PAO/GAO ratio of 1.9 ± 0.5 (Lemaire *et al.*, 2008).

The advent of molecular microbial ecology methods has enabled deeper characterization of microbiomes and optimization of wastewater treatment systems (Rittmann, 2010; Nielsen *et al.*, 2012). Similarly to activated sludge, BNR in AGS might rely on the dynamics of bacterial populations, within complex ecosystems. In order to investigate the impact of reactor characteristics and of fluctuations in operation conditions on BNR performances and bacterial community structures of AGS, a methodology combining molecular fingerprinting, amplicon pyrosequencing, bioinformatics, and numerical ecology analyses was developed. Starting from the physiological traits of the numerous bacterial populations identified, a conceptual model of the bacterial ecosystem of AGS was developed as a base for functional analyses of specific populations, and for future investigations of this fascinating biofilm microbiome with high-complexity real wastewater under pilot and full-scale conditions.

Material and methods

Reactor setups

Two lab-scale double-wall glass bubble-column SBRs (SBR-1, SBR-2) fed with synthetic wastewater were operated over 7 months under alternating anaerobic-aerobic conditions for BNR. The reactor characteristics are compiled in Supporting Information, Table S1.

The fixed 3-h SBR cycles were adapted from de Kreuk *et al.* (2005), comprised 60 min plug-flow anaerobic feeding, 110 min aeration, 3 min settling, 4 min withdrawal with a volume exchange ratio of 50%, and 3 min idle, and resulted in hydraulic retention times (HRT) of 6 h. The composition of the synthetic wastewaters was based on Weissbrodt *et al.* (2012a). During the aeration phase, the gas headspaces were recirculated with membrane vacuum pumps (KNF Neuberger AG, Switzerland) with superficial gas velocities of 0.015 m s^{-1} . DO was regulated by proportional-integral feed-back control with addition of air or dinitrogen gas with mass flow controllers (Brooks Instrument), and pH was maintained at 7.0 ± 0.3 by addition of HCl or NaOH at 1 M.

Both reactors were inoculated with precultivated mature AGS that comprised 28% of *Accumulibacter*-related PAO and 25% of *Competibacter*-related GAO, and that exhibited efficient BNR. The granular biomasses were then cultivated during a preliminary acclimation phase of 65 days up to concentrations of $18 \pm 2 \text{ g}_{\text{TSS}} \text{ L}^{-1}$ and bed heights of 30 and 35 cm, respectively, that were optimal for full uptake of acetate during the anaerobic feeding phase. The biomass concentrations and bed heights were maintained during the main experimental period of 150 days by wasting sludge manually once every 6 days at the bottom of the settled AGS beds up to day 115 and by automated purge of a fraction of the aerated mixed liquors at the column halves from this day onwards. This resulted in steady SRTs of 20 ± 3 days.

SBR-1 and SBR-2 were operated at 20 and 25 °C, respectively. This choice was motivated by the fact that this parameter can have an impact on nitrification performances as well as on the competition between PAO and GAO.

Fluctuations in operation conditions

During the main experimental period of 150 days, the fluctuations in operation conditions resulted from subsequent changes in acetate concentration, nutrient ratios, and DO setpoint over ranges (Table 1) that have been used in previous studies investigating BNR with AGS. Each parameter variation lasted over at least one SRT. According to the box plots provided in Fig. S1a, six main phases were delineated and described hereafter.

During the first 20 days (*phase 1*) following the acclimation phase, the two SBRs were operated with high concentrations of acetate and high COD/P and COD/N ratios measured in the influent wastewaters up to median values of $577 \text{ mg}_{\text{COD}} \text{ L}^{-1}$, $35.3 \text{ g}_{\text{COD}} \text{ g}_{\text{P}}^{-1}$, $12.8 \text{ g}_{\text{COD}} \text{ g}_{\text{N}}^{-1}$ for SBR-1, and $667 \text{ mg}_{\text{COD}} \text{ L}^{-1}$, $29.6 \text{ g}_{\text{COD}} \text{ g}_{\text{P}}^{-1}$, $10.4 \text{ g}_{\text{COD}} \text{ g}_{\text{N}}^{-1}$ for SBR-2. The two reactors were initially operated under moderate (60%) and high (100%) DO setpoints, respectively, according

Table 1. Ranges of fluctuations in operation variables in the two SBRs

Operation variables	Units	SBR-1	SBR-2
Acetate concentration	mg _{CODs} L ⁻¹	379–577	364–722
Volumetric OLR*	mg _{CODs} L _r ⁻¹ cycle ⁻¹	190–289	181–362
Daily volumetric OLR*	kg _{CODs} m _r ⁻³ day ⁻¹	1.5–2.3	1.4–2.9
F/M ratio*	mg _{CODs} g _{CODx} ⁻¹ cycle ⁻¹	12–18	11–29
Daily sludge loading rate*	kg _{CODs} m _{granules} ⁻³ day ⁻¹	10–15	12–24
COD/P ratio [†]	g _{CODs} g _P ⁻¹	19–46	20–35
COD/N ratio [†]	g _{CODs} g _N ⁻¹	8–13	8–12
N/P ratio [†]	g _N g _P ⁻¹	2.1–4.0	2.1–3.5
Dissolved oxygen setpoint [‡]	% O ₂ saturation	60 or 80	80 or 100

*The acetate concentration in the influent wastewater was expressed as volumetric organic loading rate (OLR), food-to-microorganism ratio (F/M) and daily sludge loading rate for comparison with ranges reported in literature, e.g. de Kreuk *et al.* (2007). These conversions were obtained by considering the 50% volume exchange ratio, the eight SBR cycles per day, the average biomass concentration of 12 g_{VSS} L_r⁻¹ (\equiv 16 g_{CODx} L_r⁻¹) and the volume of granules of 0.157 and 0.123 m_{granules}³ m_r⁻³ estimated in Table S1 for SBR-1 and SBR-2, respectively.

[†]Ratio of the concentrations of organic matter, orthophosphate, and ammonium nitrogen present in the influent wastewater.

[‡]DO setpoint applied during the aeration phases of the SBRs.

to levels assessed in fundamental studies (de Kreuk *et al.*, 2007). SBR-2 was initially operated under full aeration to avoid limitations in DO because almost twice bigger granules were observed in this reactor after the acclimation phase. Between days 20–45 (*phase 2*), the acetate concentrations were decreased from 20% in the influent of both reactors with concomitant slight decreases in the COD to nutrient ratios. Between days 45–80 (*phase 3*), both reactors were operated at an equal intermediate DO setpoint of 80%. From day 75 onwards, the reactors were operated at DO setpoints set back to the initial values of 60% and 100%, respectively. Between days 75–100 (*phase 4*), the COD/P ratios in the influent of both reactors were decreased to a value around 20 g_{COD} g_P⁻¹ that has previously been described to favour the selection of PAO over GAO in activated sludge (Schuler & Jenkins, 2003). This ratio was mainly achieved by increasing the concentration of phosphorus in the influent of SBR-1 and by decreasing the concentration of acetate in the influent of SBR-2. The reactors were operated between days 100–125 (*phase 5*) with low acetate concentration and nutrient ratios in the influent, prior to slight increases in the acetate concentration and COD/P ratio between day 125–150 (*phase 6*).

Analyses of soluble compounds and particulate biomass

Methods for the analysis of acetate, of nitrogenous and phosphorous ionic solutes, and of total (TSS), volatile (VSS) and inorganic suspended solids have been described previously in Weissbrodt *et al.* (2012a). The AGS present in the two reactors displayed significantly different particle size distributions over the whole experimental period after the acclimation phase according to daily visual observation

in the fully transparent glass reactors. A measurement of the granule size distributions (Feret's diameter) was therefore conducted after 100 days for quantitative confirmation, by light microscopy on intact granular sludge samples and digital image analysis in IMAGEJ 1.45s (NIH, 2012) according to Beun *et al.* (1999).

Molecular analyses of bacterial community compositions

AGS was sampled at an average frequency of one sample every 9 days and further conditioned for molecular analyses. Aliquots of 5 mL of AGS were homogenized in a 15-mL Potter-Elvehjem tissue grinder (Wheaton Industries Inc.). The resulting biomass suspensions were aliquoted in 1.5-mL Eppendorf tubes, pelletized by centrifugation at 18 000 g during 30 s and stored at –20 °C until analysis in batches of 16 samples.

The bacterial community compositions of AGS were investigated with high temporal resolution by community fingerprinting using terminal restriction fragment length polymorphism (T-RFLP) analysis of the v1-v3 hypervariable region of the bacterial 16S rRNA encoding gene pool. The labelled 8f and unlabelled 518r PCR primers (FAM-5'-AGAGTTTGATCMTGGCTCAG-3' and 5'-ATTACCGCGGCTGCTGG-3') and the *Hae*III endonuclease were used according to Weissbrodt *et al.* (2012a) to this end. The T-RFLP profiles were expressed as relative contributions of operational taxonomic units (OTU) and were presented in stacked bar plots of predominant OTUs (> 2%). As 16S rRNA gene copies per bacterial cell can vary from 1 to 15 (Kembel *et al.*, 2012) and the PCRs were not performed quantitatively, the percentages of OTUs determined in each sample were indicative of relative abundances only. PAO/GAO ratios were calculated

by dividing the relative abundances of the predominant OTU-214 and OTU-239 that affiliated with the phylotypes *Accumulibacter* and *Competibacter*, respectively.

The PyroTRF-ID bioinformatics methodology developed to combine T-RFLP and bacterial tag encoded FLX amplicon pyrosequencing (bTEFAP) analyses (Weissbrodt *et al.*, 2012b) was used for detailed and rational analysis of the dynamics of bacterial community composition and for high-throughput identification of dominant and low-abundance accompanying phylotypes involved. DNA was extracted from selected biomass samples collected on days 66, 84, and 114 in SBR-1, on day 125 in SBR-2, and on day 6 from AGS wasted from SBR-1. The DNA extracts were diluted to 20 ng μL^{-1} and sent to Research and Testing Laboratory LLC (Lubbock, TX) in an express (2–3 days) dry ice parcel for bTEFAP analysis according to the protocol developed by Sun *et al.* (2011).

Numerical ecology methods

Hierarchical clustering, ordination and multivariate statistical analyses of operation, BNR and T-RFLP data sets were computed in the R software (R Development Core Team, 2008) equipped with the additional packages VEGAN (Oksanen *et al.*, 2009), Heatplus (Ploner, 2011) and heatmap.plus (Day, 2007), according to the methodology detailed by Borcard *et al.* (2011), and briefly described hereafter. This multivariate numerical ecology approach enabled to consider the full complexity of operation, bacterial community and BNR data sets and to deal with simultaneous changes in several operation parameters at a time.

Hierarchical clustering analyses were computed with the Ward's minimum variance method to define major groups of daily reactor states. Principal component analyses (PCA) and multiple factor analyses (MFA) were computed to assess the relationships between the data sets and to represent their common evolution in a graphical way during reactor operation. The interconnections between data sets were displayed in group representations, the evolution of the reactor states in individual factor maps and the extent of correlations between the three data sets in correlation circles with proportional vector directions and lengths. Spearman's rank correlation coefficients, RV-coefficients (Robert & Escoufier, 1976) and *P*-values with 10 000 permutations were computed as measures of similarities to assess the statistical significance of the observed correlations. Pairwise correlations between each OTU and each operation and performance parameter were graphed in heatmaps with proportional colour intensities to detect conditions that select for clusters of OTUs.

Results

Nutrient removal performances

The dynamics in BNR performances of the two SBRs were delineated in six periods according to the main changes in operation variables during the 5-months experiments (Fig. 1). For each period, the median levels of operation and BNR parameters are compiled in the box plots provided in Fig. S1a. The global trends in reactor performances are described hereafter based on the median (*m*), first and third quartiles (*q*₁–*q*₃). After 20 days of adaptation of the reactors to fixed SRT conditions (*phase 1*), changes in DO setpoints and fluctuations in wastewater compositions impacted on BNR performances.

SBR-1 was efficiently removing phosphorus (*m* = 99%; *q*₁–*q*₃ = 97–99%) and nitrogen substantially (69%; 64–70%) during *phase 2* under the conditions with 60% DO, 447 (444–468) $\text{g}_{\text{COD}} \text{L}_{\text{Inf}}^{-1}$, 33.6 (33.3–36.3) $\text{g}_{\text{COD}} \text{g}_{\text{P}}^{-1}$ and 11.2 (11.1–11.6) $\text{g}_{\text{COD}} \text{g}_{\text{N}}^{-1}$ (Fig. 1a–b). Nitrogen removal was impaired (51%; 48–54%) during *phase 3* by the increase in DO from 60% to 80%, but punctually recovered to 70% after setting back DO to 60% in the beginning of *phase 4*. The low nutrient ratios of 19.7 (19.2–20.2) $\text{g}_{\text{COD}} \text{g}_{\text{P}}^{-1}$ and 9.0 (8.8–9.1) $\text{g}_{\text{COD}} \text{g}_{\text{N}}^{-1}$ measured in the influent wastewater after the end of *phase 4* resulted in low nitrogen removal of 49% (47–49%) during *phase 5* and *phase 6*. Under these conditions, phosphorus removal got progressively altered as well (93%; 81–94%). Acetate was fully taken up under anaerobic conditions (98.8%; 98.4–99.9%), and ammonium was fully nitrified aerobically (99.6%; 98.1–99.9%) during the whole experimental period.

In SBR-2, acetate was fully taken up anaerobically as well (98.5%; 98.1–98.8%). This reactor was efficiently nitrifying ammonium (98%; 96–98%) and removing nitrogen (82%; 81–84%) and phosphorus (99%; 98–99%) during *phase 2* with 100% DO, 556 (552–576) $\text{g}_{\text{COD}} \text{L}_{\text{Inf}}^{-1}$, 26.3 (26.1–28.3) $\text{g}_{\text{COD}} \text{g}_{\text{P}}^{-1}$ and 9.5 (9.3–9.7) $\text{g}_{\text{COD}} \text{g}_{\text{N}}^{-1}$ (Fig. 1c–d). Nitrification and phosphorus removal declined to 74% (70–84%) and 87% (78–91%), respectively, during *phase 3* after decreasing DO to 80%, but recovered in the end of *phase 4* after setting back DO to 100%. The lower acetate concentration of 376 (375–385) $\text{mg}_{\text{CODs}} \text{L}_{\text{Inf}}^{-1}$ and lower COD/P ratio of 20.8 (20.8–21.7) $\text{g}_{\text{COD}} \text{g}_{\text{P}}^{-1}$ applied during *phase 5* resulted in low removal of nitrogen (30%; 27–34%) and phosphorus (87%; 85–89%). Nitrogen removal increased again to 56% (43–59%) after a slight increase in the organic substrate concentration to 395 (384–404) $\text{mg}_{\text{COD}} \text{L}_{\text{Inf}}^{-1}$ during *phase 6*. A closer look at nitrogen-related processes

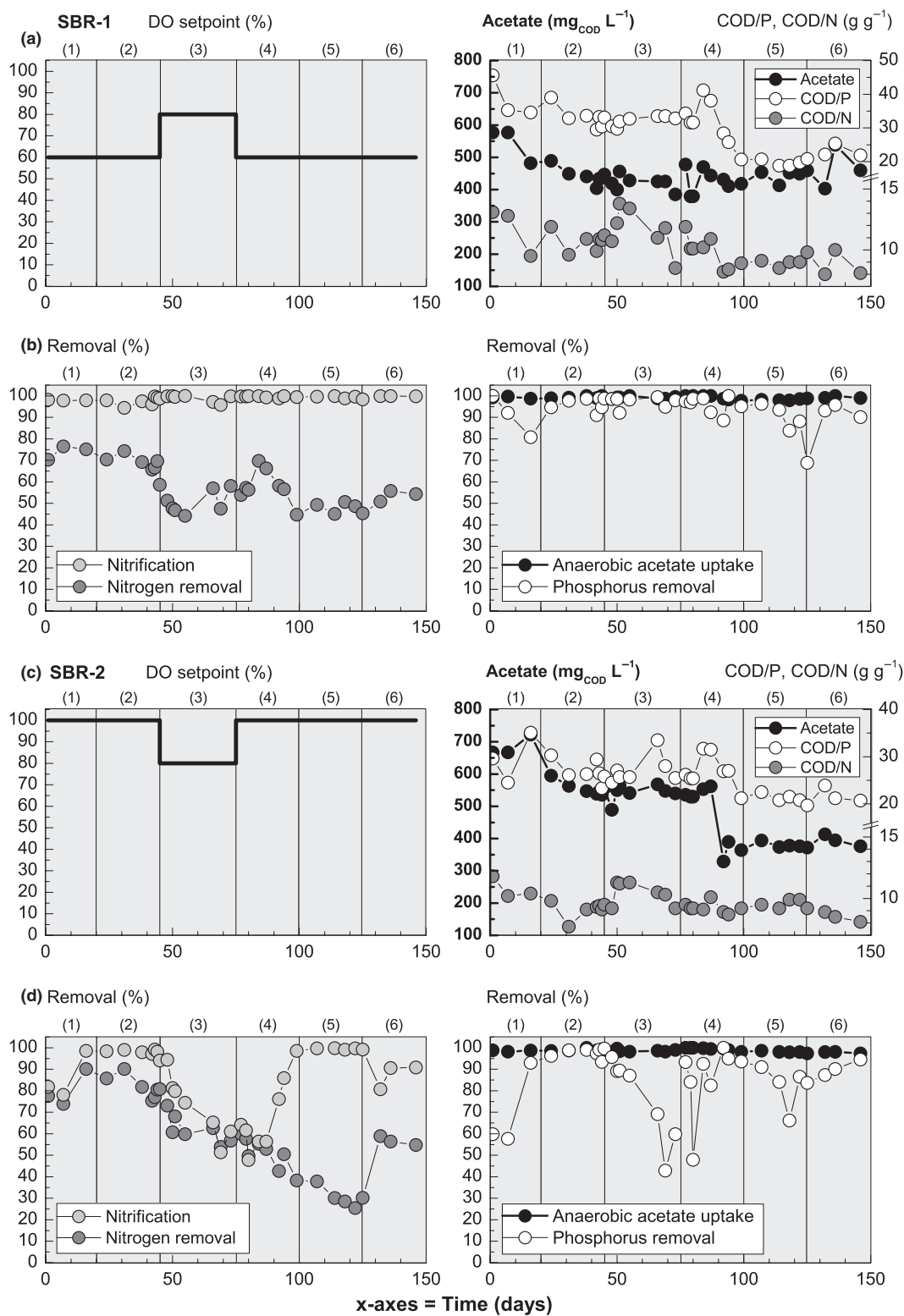


Fig. 1. Impact of switches in DO setpoints and of fluctuations in the influent compositions on the BNR performances in SBR-1 (a and b) and SBR-2 (c and d). (a and c) illustrate operating conditions. (b and d) describe the impact on nutrient removal performances. The experimental period of 150 days was delineated in 6 phases (numbers in brackets) according to the main changes in operation variables according to the box plots provided in Fig. S1a.

revealed that nitrogen removal was limited in SBR-2 by nitrification during *phases 3–4* and by denitrification during *phase 5* (Fig. S1). The concentration of nitrite was in addition considerably higher in the effluent of SBR-2 (0.6 (0.3–0.9) mg_{N-NO₂} L⁻¹) than in the effluent of SBR-1 (0.01 (0–0.01) mg_{N-NO₂} L⁻¹) over the whole experimental period. According to two-sample *t*-test ($\alpha = 0.05$), SBR-2 was globally displaying significantly different altered patterns of nitrification ($P = 0.003$) and phosphorus removal ($P = 0.02$) than SBR-1 (Fig. S1b).

In addition, according to regular daily visual observation of the reactor contents, the AGS present in SBR-2 was composed of almost twice bigger granules than the AGS of SBR-1 over the whole experimental period after the acclimation phase. A microscopy measurement on

day 100 confirmed these observations with a biofilm particle size distribution of 1.5 ± 0.9 mm in SBR-1 and of 2.9 ± 1.5 mm SBR-2.

Overall bacterial community compositions

The bacterial communities of the AGS present in the two SBRs (Fig. 2 and Table S2) were globally composed (i) of the same predominant populations present in relative abundances above 10% of the total bacterial community and affiliating with *Xanthomonadaceae* (OTU-32), *Accumulibacter* (OTU-214) and *Competibacter* (OTU-239), and (ii) of phylotypes present in moderate relative abundances (2–5%) related to *Aminobacter* (OTU-220), *Intrasporangiaceae* (OTU-223), a second population of *Accumulibacter*

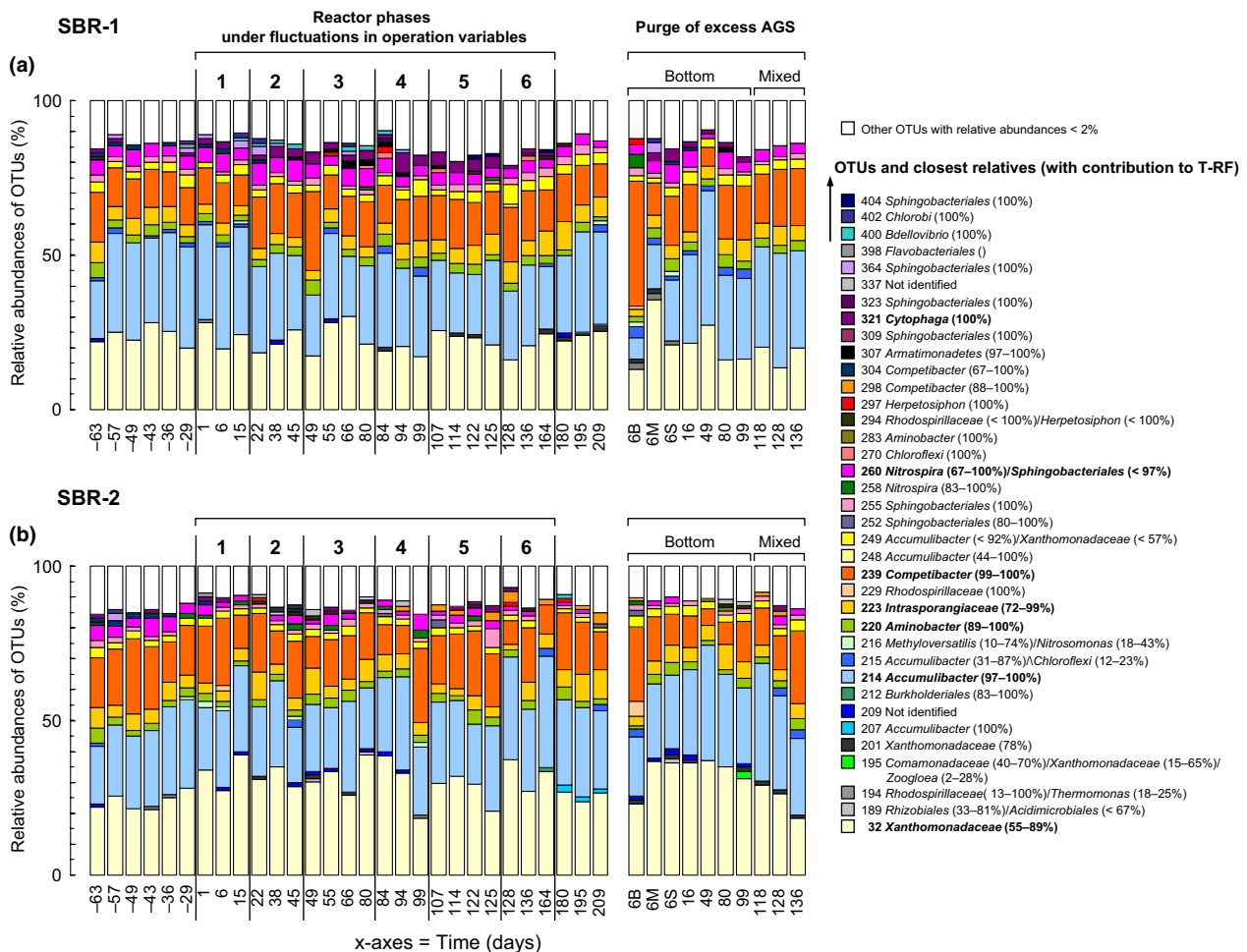


Fig. 2. Evolution of the bacterial community compositions of the AGS present in the reactors and in the purge streams during the operation of SBR-1 (a) and SBR-2 (b). The experimental period run during five months at fixed SRT under fluctuations in operation conditions was started after having cultivated substantial amounts of AGS during the initial acclimation phase of 65 days (samples –63 to –29). T-RFLP profiles of purged granules sorted by size, that is, small (< 1 mm; 6S), medium (1–3 mm; 6M) and big (3 mm; 6B) are provided on day 6. Closest bacterial affiliations obtained with PyroTRF-ID (Table S2) are given together with their relative contribution to OTUs.

(OTU-249), *Nitrospira* and *Sphingobacteriales* (OTU-260), and *Cytophaga* (OTU-321). These major populations were accompanied by numerous low-abundance (< 2%) organisms that were related either to the lineages of the dominant ones or to in different phylogenies. Four and five different OTUs were contributing to the candidate genera *Competibacter* and *Accumulibacter*, respectively. The order *Sphingobacteriales* was represented by seven different OTUs that accounted for total relative abundances of 4.2% (3.6–5.1%) in SBR-1 and 3.3% (2.6–3.8%) in SBR-2.

The AGS ecosystems of the two SBRs operated under well-defined synthetic conditions were globally related to moderate richness (SBR-1: 45, 40–48; SBR-2: 38, 35–42) and Shannon's diversity indices (SBR-1: 2.6, 2.4–2.6; SBR-2: 2.2, 2.1–2.4), based on all OTUs detected by T-RFLP. Interestingly, the AGS of SBR-1 displayed a continuous slight increase in richness from 37 (36–38) to 52 (50–54) and diversity from 2.28 (2.26–2.33) to 2.72 (2.65–2.73) over the experimental period (Fig. S1c). No such trend was observed for SBR-2.

Accumulibacter and *Competibacter* were present in comparable relative abundances of 26% (23–28%) and 14% (13–16%) in SBR-1 and 25% (21–28%) and 16% (11–18%) in SBR-2 (Fig. S1c). These two populations formed a median PAO/GAO ratio that was almost identical in SBR-1 (1.7; 1.6–2.2) and SBR-2 (1.5; 1.2–2.3). In SBR-1, this ratio evolved proportionally to the acetate load and nutrient ratios. In SBR-2, the ratio did not exhibit a clear trend in relation with nutrient loads. Populations of *Aminobacter* (2.7% vs. 2.4%) and *Intrasporangiaceae* (4.2% vs. 4.0%) were present in comparable relative abundances in both reactors, with 2.7% (2.5–3.1%) and 4.2% (3.3–5.0%) in SBR-1, and 2.4% (2.1–2.8%) and 4.0% (3.4–4.9%) in SBR-2, respectively.

Some main differences between the overall bacterial community compositions of the two systems were detected. *Xanthomonadaceae* affiliates were displaying significantly higher relative abundances in SBR-2 (31%; 28–35%) than in SBR-1 (21%; 19–25%). *Xanthomonadaceae* (33%) and *Competibacter* (18%) relatives were already relatively more abundant in SBR-2 after the preliminary period of 65 days of AGS cultivation. Conditions favouring nitrogen removal seemed to select for the *Xanthomonadaceae* population in this reactor with slightly higher relative abundances during phases 1–3 (34%; 29–37%) than during phases 4–6 (29%; 25–32%) after the decrease in the acetate concentration and nutrient ratios (Fig. S1c). Nitrite-oxidizing populations affiliating with the genus *Nitrospira* were relatively more abundant in SBR-1 (4.1%; 3.6–5.4%) than in SBR-2 (1.8%; 1.3–2.6). This might be related to the more efficient conversion of nitrite to nitrate in SBR-1. The relative abundance of the genus *Cytophaga* was also higher in the AGS of

SBR-1 (2.6%; 1.7–3.6%) than of SBR-2 (1.0%; 0.7–1.7%).

Furthermore, the PAO/GAO ratio in SBR-2 was higher (3.8 ± 2.0) in the bottom fractions of the AGS that was wasted manually between days 15–99 than in the mixed liquors (1.8 ± 0.8). In SBR-1, no evident difference was however found between the two sludge fractions. Granule size sorting on day 6 in both reactors revealed higher PAO/GAO ratios in granules smaller than 2 mm (1.3–2.5) than in larger ones (0.3–1.0). After day 115, the AGS present in the reactors and the AGS wasted automatically from the aerated mixed liquors were characterized by similar PAO/GAO ratios in a range between 1.3–3.1.

Hierarchical clustering and PCA revealed distinct behaviours of the SBRs at process scale

Hierarchical clustering of operation and BNR data sets revealed distinct behaviours of the two reactors up to day 92, but similar ones from this day onwards (Fig. S2). Bacterial community structures were grouped in the same cluster during the acclimation phase, but in distant ones under subsequent operation at fixed SRT. According to PCA, the distant initial BNR performances of SBR-1

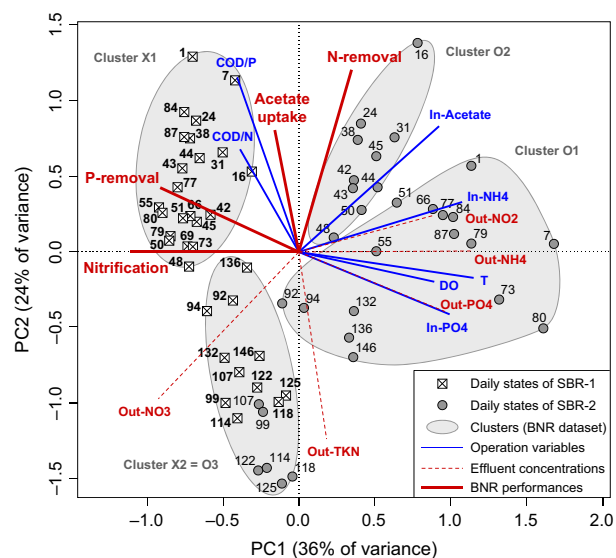


Fig. 3. Principal component analysis (PCA) of the concatenated data sets of operation variables and BNR performances of SBR-1 (white \square symbols) and SBR-2 (grey \circ symbols). The sampling days are given after each symbol. The grey ellipses represent the five main clusters (X1–X2, O1–O4) of daily reactor states obtained after hierarchical clustering analysis of the BNR data set in Fig. S2. The cluster 'X2 = O3' indicates common behaviour of both SBRs during later operation. The direction and the length of the red vectors indicate the extent of positive and inverse correlations between the operation variables and the BNR performances, including nutrient removal and residual concentrations in effluent, for each cluster of daily states.

(cluster X1) and SBR-2 (clusters O1-O2) were reflected by opposite correlations with operation variables (Fig. 3). The global vertical separation between the distinct process behaviours is explained by the phosphorus removal and nitrification vectors. The horizontal separation between initial and final reactor stages is related to the nitrogen removal vector. Higher phosphorus removal and nitrification in SBR-1 were correlated positively with the operation at higher nutrient ratios. Higher nitrogen removal was correlated with higher nutrient ratios in SBR-1 and higher acetate load in SBR-2. After day 90, both reactors exhibited similar behaviour (identical clusters X2 and O3) characterized by efficient nitrification but poor nitrogen removal (i.e. high residual nitrate concentrations). The inverse correlation between the vectors related to nitrification and phosphorus removal and the vectors related to temperature and DO indicated that these two operation variables might have impacted aerobic conversion in SBR-2.

Significance of correlations between operation, BNR and bacterial community data sets

The pairwise Spearman's rank correlation coefficients and *P*-values indicated that the operation and BNR data sets were significantly correlated for both SBRs (Table S3). BNR performances were mainly related to the orthophosphate concentration and nutrient ratios in the influent of SBR-1 and to the acetate and ammonium loads, and the COD/P ratio in the influent of SBR-2.

In SBR-1, phosphorus was efficiently removed with high DO, low orthophosphate load and high nutrient ratios. Nitrogen removal was enhanced by high acetate load and nutrient ratios. Anaerobic acetate uptake and nitrification were displaying minor fluctuations in this

reactor, and thus no significant correlation with operation variables. In SBR-2, nitrification was efficient with high DO, low acetate and ammonium loads, and low COD/P ratio. Nitrogen was efficiently removed under the opposite conditions. Only low correlations were obtained for phosphorus removal. As the COD/N ratio displayed less variation in the influent wastewater of SBR-2 than of SBR-1 (Fig. S1a), this parameter was related to less significant impact on the concentrations of nitrate in the treated effluent of the second reactor.

Globally, the group representations provided in Fig. 4 indicate that the bacterial community dynamics were significantly related to the fluctuations in operation conditions and BNR performances in SBR-1, whereas the operation dynamics had only a direct effect on BNR in SBR-2 without identified significant impact at bacterial community level. Significant correlations between bacterial community structures and almost all operation and BNR parameters, except DO and anaerobic acetate uptake, were indeed only obtained for SBR-1 (Table S4). The underlying community compositions were significantly correlated with the orthophosphate load and nutrient ratios and with nitrogen removal.

Identification of bacterial relatives sharing similar behaviour

A MFA was then conducted on the three data sets related to SBR-1 to detect correlations between the dynamics of both predominant and low-abundance accompanying bacterial relatives and the fluctuations in operation variables and BNR performances in this reactor (Fig. S3). The stable acetate uptake and nitrification performances were not considered in the MFA. Starting from the group representation (Fig. S3a), the combination of the

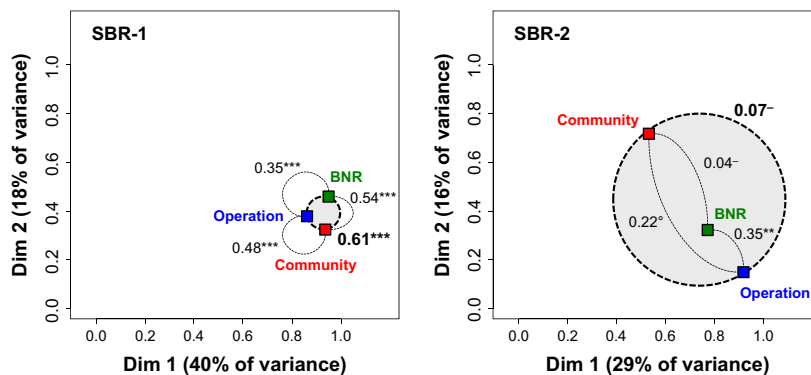


Fig. 4. Group representation of the degree of interconnection in the statistical space between the dynamics in operation conditions, BNR performances and bacterial community structures of the two SBRs. The closer the points are, the higher are the data sets connected. Pairwise Spearman's rank correlation coefficients between the data sets are in addition provided next to the light dashed connectors and are accompanied by significance codes of *P*-values (i.e.: highly significant: 0*** 0.001 ** 0.01 * 0.05 ° 0.1–1: not significant). The global rank correlation coefficient between the three data sets is provided in bold together with the bold dashed grey circle.

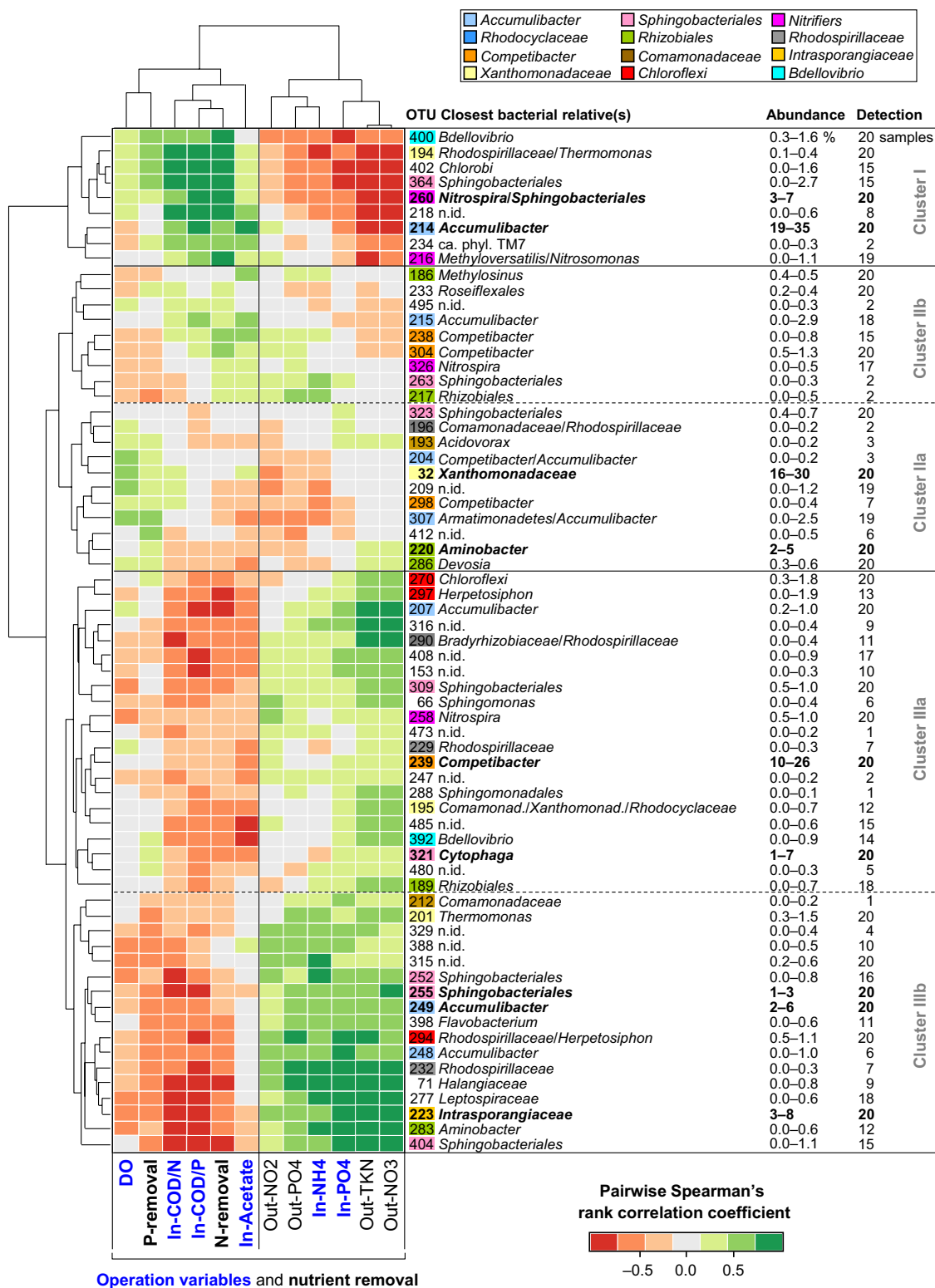


Fig. 5. Heat map of the pairwise Spearman's rank correlations between OTUs and operation and BNR parameters in SBR-1. The top dendrogram defines clusters of operation and BNR parameters correlating with each other. The left dendrogram defines clusters of OTUs sharing similar correlations with operation and BNR parameters. Each OTU is given with the closest bacterial affiliation(s), with the minimum–maximum range of relative abundance, and the number over a maximum of 20 samples in which the OTU was detected.

individual factor map representing the evolution of the daily reactor states in the statistical space with the clusters of daily bacterial community composition revealed a structuring of community dynamics in three successive periods (Fig. S3b–c). Correlation circles allowed identifying correlations between these periods, the operation variables, the BNR performances and the specific OTUs according to vector lengths and directions (Fig. S2c).

The heatmap presented in Fig. 5 provides a compact view of the clusters of dominant and accompanying phylotypes that shared similar pairwise correlations with single operation variables and BNR performances. This multivariate analysis revealed that the AGS bacterial community continuum was composed of two main antagonistic bacterial clusters I and III, and one transitory cluster II. The phylotypes of cluster I were favoured under conditions selecting for enhanced BNR (i.e. P-removal > 95% and N-removal > 65%), whereas the phylotypes of cluster III were favoured under the opposite conditions (i.e. P-removal < 90% and N-removal < 60%).

The conditions of high acetate load and nutrient ratios during the first 40 days resulted in efficient nitrogen removal and selected for cluster I composed of predominant *Accumulibacter* and *Nitrospira* relatives accompanied by populations of *Bdellovibrio*, *Thermomonas*, *Methyloversatilis* and *Nitrosomonas*. The high DO conditions of the next period up to day 100 resulted in efficient phosphorus removal but less efficient nitrogen removal and selected for *Xanthomonadaceae* and *Aminobacter* relatives inside the subcluster IIa and lower relative abundances of accompanying populations of *Accumulibacter*, *Competibacter*, *Nitrospira*, *Sphingobacteriales*, *Armatimonadetes* and *Rhizobiales* inside the subcluster IIb. The conditions of low acetate load and nutrient ratios over the last 50 days correlated with low BNR performances and higher relative abundances in bacterial relatives belonging to cluster III. The subcluster IIIa comprised predominant *Competibacter* and *Sphingobacteriales*-related *Cytophaga* affiliates and accompanying populations of *Chloroflexi*, *Accumulibacter*, *Rhodospirillaceae*, *Nitrospira* and *Rhizobiales* relatives. The subcluster IIIb comprised *Intrasporangiaceae* relatives, *Accumulibacter* and *Sphingobacteriales* affiliates, and accompanying populations of *Thermomonas*, *Rhodospirillaceae* and *Aminobacter*.

Discussion

Wastewater treatment systems are designed for operation on long term with variations in influent wastewater composition and environmental conditions that might affect the process performances. Based on experiments conducted with defined synthetic wastewater

compositions, this study provides valuable insights on the impact of operation variables and their fluctuations on BNR performances, bacterial community structures and dynamics of target phylotypes in AGS. This knowledge is a useful basis for defining bacterial resource management strategies at pilot and full scale. The combination of classical and high-throughput molecular methods with numerical ecology approaches was dedicated to the identification of multilevel correlations from the macro- to the microscales.

Optimal bacterial selection under stable SRT

In conventional activated sludge systems, fine tuning of the SRT is required for efficient bacterial selection and BNR performances. One advantage of using AGS biofilms instead of flocs is the achievement of higher biomass concentrations and longer sludge ages. Operating AGS-SBRs without control of the SRT can however lead to impaired bacterial selection and process disturbances (de Kreuk *et al.*, 2007; Gonzalez-Gil & Holliger, 2011; Weissbrodt *et al.*, 2013a). Maintaining the SRT at 20 days by wasting sludge periodically led to effective phosphorus removal and stable overall bacterial community compositions. The average PAO/GAO ratios met the level reported by Lemaire *et al.* (2008) for efficient phosphorus removal. Wasting sludge either from lower settled bed fractions or from aerated mixed liquors did not lead to different impacts on community structures. Decreasing gradients in granule size and PAO/GAO ratio have previously been observed along AGS beds, and PAO have been preferentially selected by purging upper bed fractions (Winkler *et al.*, 2011; Bassin *et al.*, 2012). Here, no clear gradients were observed. *Accumulibacter* was only more abundant in bottom bed fractions of SBR-2. Such gradients might therefore be system specific. Overall, similarly to other biofilm systems (Morgenroth & Wilderer, 1999), controlled biomass removal is required for optimal selection and phosphorus removal in AGS.

Bed volume and granule size impact on the oxygenation of AGS

Despite operation at optimal SRT and rather high DO, the two reactors displayed different behaviours in aerobic processes of nitrification and phosphorus removal. Full and stable nitrification was indeed constantly measured over the experimental period in the first SBR operated at 20 °C independent of the DO setpoint applied (60–80%). In the second SBR, operating at 25 °C, the ammonium oxidation dropped from 100% to <60% as soon as the DO setpoint was decreased from 100% to 80%. Based on the physiology of nitrifiers and

on the extended knowledge gained from nitrification in activated sludge systems, this differences in nitrification performances observed at 20 and 25 °C remained puzzling because nitrification should have been more efficient at 25 than at 20 °C (Wild *et al.*, 1971; Ekama & Wentzel, 2008). Temperature should thus be excluded as a factor explaining this observation.

As the AGS in the two reactors exhibited significantly distinct particle size distributions over the whole experimental period, an analysis of the three-phase AGS systems was conducted here and highlighted that the aerobic processes were most probably affected in SBR-2 by limited mass transfer at both gas–liquid and liquid–biofilm interfaces (Table S1). Floc and biofilm properties have previously been reported to impact on the mass transfer of solutes such as DO from the liquid phase to bacterial cells (Meyer *et al.*, 2003; Manser *et al.*, 2005; Filali *et al.*, 2012).

At the gas–liquid interface, the measured volumetric mass transfer coefficients ($k_{L,a}$) of oxygen were two and five times lower than the theoretical values computed at 20 and 25 °C based on Heijnen & Van't Riet (1984). However, the transfer should have been more efficient at higher temperature (Vogelaar *et al.*, 2000). The size and amount of solid particles and the liquid height to reactor diameter ratio (H_L/D) can affect the gas–liquid transfer in shallow bubble columns by increasing coalescence (Mena *et al.*, 2005; Lau *et al.*, 2010). As this effect is inversely proportional to the particle size, the lower oxygen mass transfer measured in SBR-2 can be related to higher H_L/D and bigger volume of granular biomass. In this reactor, the interfacial biofilm surface area was in addition twice lower as a consequence of bigger granule sizes that might be explained by initial operation at higher organic load (Moy *et al.*, 2002; Weissbrodt *et al.*, 2013b).

On the nitrification perspective, this study shows that the physiological positive effect of a higher mesophilic temperature might be counteracted by the size distribution and the amount of granular biofilms present in the AGS-SBR. Although granule size and shape are hardly controllable (de Kreuk *et al.*, 2007), periodical measurement of these parameters could allow for feedback process control towards efficient BNR.

Impact of fluctuations in operation variables in AGS systems

Relatively to the encountered fluctuation ranges of wastewater composition, heterotrophic BNR processes were efficient in AGS with noncarbon-limited conditions with at least 500 mg_{COD} L⁻¹, 30 g_{COD} g_P⁻¹ and 10 g_{COD} g_N⁻¹. At such acetate concentration, the sludge loading rate was above 14 kg_{CODs} day⁻¹ m⁻³_{granules} and was meeting the

minimal requirement reported by de Kreuk *et al.* (2007) for efficient BNR. When compared to the stoichiometric analysis of Kuba *et al.* (1996) of simultaneous and separate phosphorus removal and denitrification processes in activated sludge, an acetate supply below 500 mg_{CODs} L⁻¹ would have been sufficient for anoxic phosphorus removal, but limiting for separate processes, from an influent composed of 2–4 g_N g_P⁻¹. According to the limited performances measured at lower concentrations, phosphorus and nitrogen removal might have not been carried out by only PAO in AGS.

COD/P ratios of 20 and 200 g_{COD} g_P⁻¹ have typically been used to enrich for *Accumulibacter* and *Competibacter*, respectively, in activated sludge (Oehmen *et al.*, 2007). *Competibacter* was able here to compete with *Accumulibacter* even at ratios below 30 g_{COD} g_P⁻¹. Schuler & Jenkins (2003) have considered the PAO/GAO competition on a continuum of the two metabolisms along the COD/P axis. Nonlimited organic conditions with ratios above 25 g_{COD} g_P⁻¹ have been recommended for safe phosphorus removal.

Higher nitrogen removal in SBR-1 at lower DO might rely on decreased penetration of DO in granules (Manser *et al.*, 2005; Mosquera-Corral *et al.*, 2005; Volcke *et al.*, 2012). Granules of 1.2–1.4 mm and specific biofilm surface areas of 600–700 m² m_r⁻³ have been optimal for balanced aerobic and anoxic processes with 2 mg_{O2} L⁻¹ according to the mathematical modelling study of de Kreuk *et al.*, 2007. Granule sizes and interfacial areas in this reactor fitted with these ranges (1.5 ± 0.9 mm and 628 m² m_r⁻³, Table S1). Under the AGS characteristics of SBR-1, Oxygen might therefore be considerably saved with the application of a DO setpoint at least twice lower than 60% (5.5 mg_{O2} L⁻¹). Oxygenation strategies should nevertheless integrate impacts on phosphorus removal, because a positive correlation was detected between this process and DO.

A structured bacterial community continuum

The numerical ecology approach was efficient (i) for structuring the operation, BNR, and bacterial community data sets, (ii) for detecting multilevel correlations, (iii) for highlighting clusters of phylotypes sharing common behaviour, and (iv) for identifying the conditions that select for them. Statistical computations have previously been used to relate complex T-RFLP and pyrosequencing fingerprints to operation conditions (Rees *et al.*, 2004; Wang *et al.*, 2012).

Multivariate statistical investigations revealed impacts of fluctuations in operation conditions on the bacterial community structures of SBR-1. Under such fluctuating conditions, the richness and diversity of the community

underlying the AGS present in this reactor were shown to continuously increase slightly along operation. Fluctuating conditions in wastewater treatment plants have indeed been shown to lead to more diverse, robust and resilient microbial communities (Curtis & Craine, 1998). In contrast, the mass transfer limitations detected in SBR-2 could explain the low correlations between bacterial community structures and BNR efficiencies found for this reactor. Under mass transfer limitations, populations present in granular biofilms might not rapidly sense fluctuations in environmental variables.

The bacterial community continuum was composed of two major antagonistic clusters. Conditions favouring BNR (i.e. P-removal > 95%, N-removal > 65%) selected for polyphosphate-accumulating populations of *Accumulibacter* and nitrifying populations of *Nitrosomonas* and *Nitrospira*. On the contrary, conditions leading to altered BNR (i.e. P-removal < 90%, N-removal < 60%) selected for *Competibacter*, *Sphingobacteriales*, *Cytophaga* and *Intrasporangiaceae* relatives. *Sphingobacteriales* affiliates are widely present in activated sludge plants and metabolize macromolecules such as polysaccharides and proteins (Kirchman, 2002). The abundant extracellular polymeric substances (EPS) present in granular biofilms have been suspected to favour their establishment in AGS (Weissbrodt *et al.*, 2013a). Interestingly, *Intrasporangiaceae* affiliates, such as the glucose-fermenting and polyphosphate-accumulating *Tetrasphaera* spp. (Nielsen *et al.*, 2012), have been reported to cope with conditions selecting for *Competibacter* (Weissbrodt *et al.*, 2013b).

Populations of *Xanthomonadaceae* and *Aminobacter* sp. were present in the AGS ecosystem independently of operation conditions. *Xanthomonadaceae* belong to the denitrifying community of activated sludge and AGS systems can produce exopolysaccharides (Dow *et al.*, 2003; Thierry *et al.*, 2004; Adav *et al.*, 2010). *Aminobacter* sp. inside *Rhizobiales* can accumulate poly- β -hydroxyalcanonates and reduce nitrate to nitrite (Urakami *et al.*, 1992; Kondo *et al.*, 2009). According to denitrifying and exopolysaccharide-producing physiological properties, these populations might therefore play an important role in the microbiomes of AGS biofilms. The higher relative abundances of gammaproteobacterial *Xanthomonadaceae* (e.g. *Thermomonas*, *Pseudoxanthomonas*) and *Competibacter* affiliates at 25 °C met with physiological descriptions provided in literature for these organisms (Thierry *et al.*, 2004; Lopez-Vazquez *et al.*, 2009a). *Aminobacter* sp. and members of the order *Rhizobiales* are in addition able to degrade xenobiotic substances such as estradiols and ethylenediaminetetraacetic acid (EDTA) (Bucheli-Witschel & Egli, 2001; Yu *et al.*, 2007; Yuan & VanBriesen, 2008). The synthetic wastewater adopted from de Kreuk *et al.* (2005) contained a trace element solution with EDTA as

chelating agent in relatively high amounts. The influent wastewater thus contained up to 50 mg_{EDTA} L⁻¹ which corresponds to around 50 mg_{COD} L⁻¹ and 5 mg_N L⁻¹, that is, about 10% of the chemical oxygen demand and nitrogen equivalents fed into the reactors. Ion chromatography analyses displayed full removal of EDTA, essentially during the aeration phases of both anaerobic-aerobic SBRs (data not shown). The underlying mechanism might thus be related to biological degradation rather than sorption phenomena. Bacterial populations such as *Rhizobiales* present in the microbiome of AGS biofilms could have used EDTA as an additional source of carbon and nitrogen. The high biomass concentration of 12 g_{VSS} L_r⁻¹, the high SRT imposed on 20 ± 3 days and the combination of redox conditions in these biofilm reactors could have triggered the removal of this rather recalcitrant compound. In the wastewater treatment perspective (Alder *et al.*, 1990; Joss *et al.*, 2008; Kaparullina *et al.*, 2011; Barber *et al.*, 2013; Falas *et al.*, 2013), this might confer an additional advantage to AGS for the biodegradation of organic micropollutants in addition to BNR.

The low-abundant accompanying populations were heterogeneously distributed among the different clusters identified by MFA. Other *Accumulibacter*, *Competibacter*, *Sphingobacteriales* and *Aminobacter* relatives were found in the antagonistic clusters. Some flanking populations were mainly affiliated to one particular cluster. *Chlorobi*, *Methyloversatilis*, nitrogen-fixing *Rhizobiales* (*Methylosinus*, *Devosia*), *Roseiflexales*, denitrifying *Comamonadaceae* (*Acidovorax*), *Armatimonadetes* and TM7 relatives affiliated with the 'Accumulibacter cluster'. *Chloroflexi* (*Herpetosiphon*, *Anaerolineae*), *Rhodospirillaceae*, *Flavobacterium*, *Halangiaceae* and *Leptospiraceae* populations affiliated with the 'Competibacter cluster'. *DeFluviicoccus* spp. inside *Rhodospirillaceae* has for instance been reported as a putative alphaproteobacterial GAO (Meyer *et al.*, 2006; Nielsen *et al.*, 2010). The fact that *Accumulibacter* and *Competibacter* can be composed of different clades with different aerobic and anoxic metabolisms (Oehmen *et al.*, 2010b) can explain the presence of multiple OTUs related to these organisms. Additional research on fine-scale dynamics of different clades would require the use of molecular methods targeting functional genes (Kim *et al.*, 2010; Slater *et al.*, 2010; Gonzalez-Gil & Holliger, 2011).

A conceptual model of the granular sludge ecosystem

The bacterial communities of the AGS systems operated under alternance of anaerobic and aerobic conditions were composed of predominant and flanking populations that belonged to the core microbiome of activated sludge of full-scale BNR systems (Nielsen *et al.*, 2012; Wang

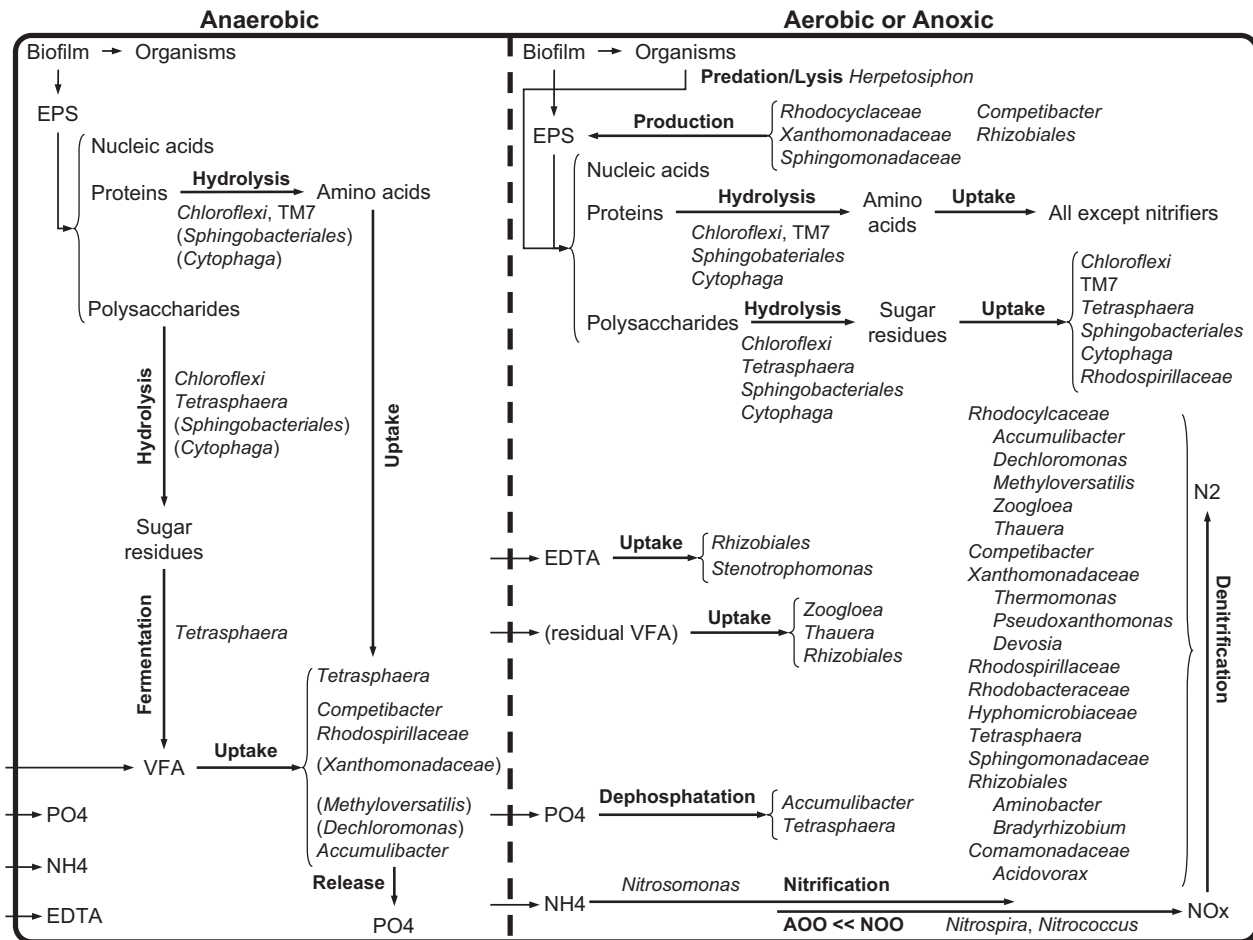


Fig. 6. Conceptual model of the granular sludge bacterial ecosystem from SBRs operated for full BNR under alternating anaerobic–aerobic conditions with VFA-based synthetic wastewater, as base for further functional analyses. The model was developed by analogy to Nielsen *et al.* (2010) starting from the numerous phylotypes identified here and in a previous study (Weissbrodt *et al.*, 2013a) with 16S rRNA gene-targeted PyroTRF-ID analysis and from their physiological traits reported in literature. The physiologies of populations displayed in brackets remain to be confirmed. Bacterial conversion processes are displayed with thick arrows. Phosphorus and nitrogen uptake for anabolic requirements are not represented. Populations other than the traditional PAO (e.g. *Accumulibacter*) and GAO (e.g. *Competibacter*) that are selected by alternating anaerobic feast and aerobic starvation conditions might be involved in phosphorus removal, denitrification and metabolism of EPS. EDTA was present in relatively high amounts in the synthetic wastewater, and consumption of this compound was observed. Additional legend: ammonium (NH₄), dinitrogen (N₂), nitrite and nitrate (NO_x), orthophosphate (PO₄).

et al., 2012). Part of the organisms detected here has also been present in other AGS systems operated for BNR (Adav *et al.*, 2010; Ebrahimi *et al.*, 2010). According to Nielsen *et al.* (2012), the dynamics resulting from alternating anaerobic–aerobic conditions select for versatile populations active during the various reactor phases. A conceptual model of bacterial interactions within the core microbiome of activated sludge has been developed (Nielsen *et al.*, 2010). An analogue conceptual model was developed here starting from the physiological traits reported in literature in order to draw the ecological relationships between the numerous phylotypes identified with PyroTRF-ID and to propose a base for future analy-

sis of functions of specific populations in the granular sludge biofilm ecosystem (Fig. 6). This ecological model highlighted the presence (i) of a putatively broad denitrifying community that might not be restricted to only *Accumulibacter* and *Competibacter* under alternating anaerobic–aerobic conditions and (ii) of populations involved in the metabolism of EPS. Based on this model, research targeting functional analyses should therefore be conducted to unravel the involvement of specific bacterial populations in BNR processes and to determine how these putative denitrifiers and EPS producers and consumers can thrive in the anaerobic–aerobic granular sludge ecosystem where the volatile fatty acid (VFA)

carbon source is fully taken up during the anaerobic phase. Proper management of the bacterial resource in wastewater treatment systems has been recommended by considering a bacterial community as a cooperative continuum (Verstraete *et al.*, 2007). Although operation under defined synthetic conditions induces a decrease in the bacterial diversity (Weissbrodt *et al.*, 2013a), the number of low-abundant flanking populations detected here demonstrated that the bacterial AGS ecosystem is composed of a complex multispecies community continuum. Deeper insights in population functions and interactions in such complex microbiomes can then be obtained with the combination of novel molecular techniques such as reviewed very recently by Vanwonterghem *et al.* (2014).

Conclusion and outlook

Operating anaerobic-aerobic granular sludge biofilm systems for BNR under steady-state conditions at a moderate SRT of 20 days is crucial for stabilizing the underlying overall bacterial community. Fluctuations in operation variables were shown to impact on BNR and on bacterial community structures depending on the efficiency of oxygenation of the granular biofilms. Heterotrophic microbial processes of phosphorus removal and denitrification were efficient under nonlimiting organic load conditions. Under nonlimiting oxygenation conditions, the structure of the bacterial community of AGS was identified with two major antagonistic clusters of both predominant and low-abundance flanking populations, according to correlations between their dynamics and the fluctuations in operation and BNR parameters. The numerous phylotypes identified in AGS belong to the core bacteriome of BNR activated sludge processes. The conceptual model of the bacterial ecosystem of AGS that was developed in this study based on their physiological traits can be used in near future as an excellent base for investigations at the functional level within the full microbial complexity of systems operated for high-rate BNR from real wastewater.

Acknowledgements

This study was financed by the Swiss National Science Foundation, Grants no. 205321-120536 and 200020-138148. The authors acknowledge Scot E. Dowd and the Research and Testing Laboratory (Lubbock) for pyrosequencing analyses, as well as François Gillet (Université de Franche-Comté, France) and Daniel Borcard (Université de Montréal, Canada) for advice on numerical ecology. The authors declare that they have no competing interests.

References

- Adav SS, Lee DJ & Lai JY (2010) Microbial community of acetate utilizing denitrifiers in aerobic granules. *Appl Microbiol Biotechnol* **85**: 753–762.
- Alder AC, Siegrist H, Gujer W & Giger W (1990) Behaviour of NTA and EDTA in biological wastewater treatment. *Water Res* **24**: 733–742.
- Barber LB, Keefe SH, Brown GK, Furlong ET, Gray JL, Kolpin DW, Meyer MT, Sandstrom MW & Zaugg SD (2013) Persistence and potential effects of complex organic contaminant mixtures in wastewater-impacted streams. *Environ Sci Technol* **47**: 2177–2188.
- Bassin JP, Winkler MKH, Kleerebezem R, Dezotti M & van Loosdrecht MCM (2012) Improved phosphate removal by selective sludge discharge in aerobic granular sludge reactors. *Biotechnol Bioeng* **109**: 1919–1928.
- Beun JJ, Hendriks A, van Loosdrecht MCM, Morgenroth E, Wilderer PA & Heijnen JJ (1999) Aerobic granulation in a sequencing batch reactor. *Water Res* **33**: 2283–2290.
- Borcard D, Gillet F & Legendre P (2011) *Numerical Ecology with R*. Springer-Verlag GmbH, Heidelberg.
- Bucheli-Witschel M & Egli T (2001) Environmental fate and microbial degradation of aminopolycarboxylic acids. *FEMS Microbiol Rev* **25**: 69–106.
- Crocetti GR, Banfield JF, Keller J, Bond PL & Blackall LL (2002) Glycogen-accumulating organisms in laboratory-scale and full-scale wastewater treatment processes. *Microbiology* **148**: 3353–3364.
- Curtis TP & Craine NG (1998) The comparison of the diversity of activated sludge plants. *Water Sci Technol* **37**: 71–78.
- Day A (2007) heatmap.plus: Heatmaps with more sensible behavior. R package version 1.3. R Foundation for Statistical Computing, Vienna, Austria. Available at: <http://cran.r-project.org/web/packages/heatmap.plus/index.html>.
- de Kreuk MK & van Loosdrecht MCM (2004) Selection of slow growing organisms as a means for improving aerobic granular sludge stability. *Water Sci Technol* **49**: 9–17.
- de Kreuk MK, Heijnen JJ & van Loosdrecht MCM (2005) Simultaneous COD, nitrogen, and phosphate removal by aerobic granular sludge. *Biotechnol Bioeng* **90**: 761–769.
- de Kreuk MK, Picioreanu C, Hosseini M, Xavier JB & van Loosdrecht MCM (2007) Kinetic model of a granular sludge SBR: influences on nutrient removal. *Biotechnol Bioeng* **97**: 801–815.
- Dow JM, Crossman L, Findlay K, He YQ, Feng JX & Tang JL (2003) Biofilm dispersal in *Xanthomonas campestris* is controlled by cell-cell signaling and is required for full virulence to plants. *P Natl Acad Sci USA* **100**: 10995–11000.
- Ebrahimi S, Gabus S, Rohrbach-Brandt E, Hosseini M, Rossi P, Maillard J & Holliger C (2010) Performance and microbial community composition dynamics of aerobic granular sludge from sequencing batch bubble column reactors operated at 20 °C, 30 °C, and 35 °C. *Appl Microbiol Biotechnol* **87**: 1555–1568.

- Ekama GA & Wentzel MC (2008) Nitrogen removal. *Biological wastewater treatment: Principles, Modelling and Design*, (Henze M, van Loosdrecht MCM, Ekama GA & Brdjanovic D, eds), pp. 87–138. IWA Publishing, London.
- Falás P, Longree P, La Cour Jansen J, Siegrist H, Hollender J & Joss A (2013) Micropollutant removal by attached and suspended growth in a hybrid biofilm-activated sludge process. *Water Res* **47**: 4498–4506.
- Filali A, Bessiere Y & Sperandio M (2012) Effects of oxygen concentration on the nitrifying activity of an aerobic hybrid granular sludge reactor. *Water Sci Technol* **65**: 289–295.
- Gonzalez-Gil G & Holliger C (2011) Dynamics of microbial community structure and enhanced biological phosphorus removal of propionate- and acetate-cultivated aerobic granules. *Appl Environ Microbiol* **77**: 8041–8051.
- Heijnen JJ & Van't Riet K (1984) Mass transfer, mixing and heat transfer phenomena in low viscosity bubble column reactors. *Chem Eng J* **28**: B21–B42.
- Hesselmann RPX, Werlen C, Hahn D, van der Meer JR & Zehnder AJB (1999) Enrichment, phylogenetic analysis and detection of a bacterium that performs enhanced biological phosphate removal in activated sludge. *Syst Appl Microbiol* **22**: 454–465.
- Joss A, Siegrist H & Ternes TA (2008) Are we about to upgrade wastewater treatment for removing organic micropollutants? *Water Sci Technol* **57**: 251–255.
- Kaparullina EN, Doronina NV & Trotsenko YA (2011) Aerobic degradation of ethylenediaminetetraacetate (review). *Appl Biochem Microbiol* **47**: 460–473.
- Kembel SW, Wu M, Eisen JA & Green JL (2012) Incorporating 16S gene copy number information improves estimates of microbial diversity and abundance. *PLoS Comput Biol* **8**: e1002743.
- Kim JM, Lee HJ, Kim SY, Song JJ, Park W & Jeon CO (2010) Analysis of the fine-scale population structure of “*Candidatus Accumulibacter phosphatis*” in enhanced biological phosphorus removal sludge, using fluorescence *in situ* hybridization and flow cytometric sorting. *Appl Environ Microbiol* **76**: 3825–3835.
- Kirchman DL (2002) The ecology of *Cytophaga-Flavobacteria* in aquatic environments. *FEMS Microbiol Ecol* **39**: 91–100.
- Kishida N, Kim J, Tsuneda S & Sudo R (2006) Anaerobic/oxic/anoxic granular sludge process as an effective nutrient removal process utilizing denitrifying polyphosphate-accumulating organisms. *Water Res* **40**: 2303–2310.
- Kondo T, Tsuneda S, Ebie Y, Inamori Y & Xu K (2009) Characterization of the microbial community in the anaerobic/oxic/anoxic process combined with sludge ozonation and phosphorus adsorption. *J Water Environ Technol* **7**: 155–162.
- Kuba T, van Loosdrecht MCM & Heijnen JJ (1996) Phosphorus and nitrogen removal with minimal COD requirement by integration of denitrifying dephosphatation and nitrification in a two-sludge system. *Water Res* **30**: 1702–1710.
- Lau R, Mo R & Beverly Sim WS (2010) Bubble characteristics in shallow bubble column reactors. *Chem Eng Res Des* **88**: 197–203.
- Lemaire R, Yuan Z, Blackall LL & Crocetti GR (2008) Microbial distribution of *Accumulibacter* spp. and *Competibacter* spp. in aerobic granules from a lab-scale biological nutrient removal system. *Environ Microbiol* **10**: 354–363.
- Lochmatter S, Gonzalez-Gil G & Holliger C (2013) Optimized aeration strategies for nitrogen and phosphorus removal with aerobic granular sludge. *Water Res* **47**: 6187–6197.
- Lopez-Vazquez CM, Hooijmans CM, Brdjanovic D, Gijzen HJ & van Loosdrecht MCM (2009a) Temperature effects on glycogen accumulating organisms. *Water Res* **43**: 2852–2864.
- Lopez-Vazquez CM, Oehmen A, Hooijmans CM, Brdjanovic D, Gijzen HJ, Yuan Z & van Loosdrecht MCM (2009b) Modeling the PAO-GAO competition: effects of carbon source, pH and temperature. *Water Res* **43**: 450–462.
- Manser R, Gujer W & Siegrist H (2005) Consequences of mass transfer effects on the kinetics of nitrifiers. *Water Res* **39**: 4633–4642.
- Mena PC, Pons MN, Teixeira JA & Rocha FA (2005) Using image analysis in the study of multiphase gas absorption. *Chem Eng Sci* **60**: 5144–5150.
- Meyer RL, Saunders AM, Zeng RJ, Keller J & Blackall LL (2003) Microscale structure and function of anaerobic-aerobic granules containing glycogen accumulating organisms. *FEMS Microbiol Ecol* **45**: 253–261.
- Meyer RL, Saunders AM & Blackall LL (2006) Putative glycogen-accumulating organisms belonging to the *Alphaproteobacteria* identified through rRNA-based stable isotope probing. *Microbiology* **152**: 419–429.
- Morgenroth E & Wilderer PA (1999) Controlled biomass removal – The key parameter to achieve enhanced biological phosphorus removal in biofilm systems. *Water Sci Technol* **39**: 33–40.
- Mosquera-Corral A, de Kreuk MK, Heijnen JJ & van Loosdrecht MCM (2005) Effects of oxygen concentration on N-removal in an aerobic granular sludge reactor. *Water Res* **39**: 2676–2686.
- Moy BYP, Tay JH, Toh SK, Liu Y & Tay STL (2002) High organic loading influences the physical characteristics of aerobic sludge granules. *Lett Appl Microbiol* **34**: 407–412.
- Nielsen PH, Mielczarek AT, Kragelund C, Nielsen JL, Saunders AM, Kong Y, Hansen AA & Vollertsen J (2010) A conceptual ecosystem model of microbial communities in enhanced biological phosphorus removal plants. *Water Res* **44**: 5070–5088.
- Nielsen PH, Saunders AM, Hansen AA, Larsen P & Nielsen JL (2012) Microbial communities involved in enhanced biological phosphorus removal from wastewater – a model system in environmental biotechnology. *Curr Opin Biotechnol* **23**: 452–459.

- NIH (2012) *IMAGEJ, Image Processing and Analysis in Java*. National Institutes of Health (NIH), Bethesda, MD.
- Oehmen A, Lemos PC, Carvalho G, Yuan Z, Keller J, Blackall LL & Reis MAM (2007) Advances in enhanced biological phosphorus removal: from micro to macro scale. *Water Res* **41**: 2271–2300.
- Oehmen A, Carvalho G, Lopez-Vazquez CM, van Loosdrecht MCM & Reis MAM (2010a) Incorporating microbial ecology into the metabolic modelling of polyphosphate accumulating organisms and glycogen accumulating organisms. *Water Res* **44**: 4992–5004.
- Oehmen A, Lopez-Vazquez CM, Carvalho G, Reis MAM & van Loosdrecht MCM (2010b) Modelling the population dynamics and metabolic diversity of organisms relevant in anaerobic/anoxic/aerobic enhanced biological phosphorus removal processes. *Water Res* **44**: 4473–4486.
- Oksanen J, Kindt R, Legendre P, O'Hara B, Simpson GL, Solymos P, Stevens MHH & Wagner H (2009) *VEGAN: Community ecology package*. R package version 1.15-4. R Foundation for Statistical Computing, Vienna, Austria. Available at: <http://CRAN.R-project.org/package=vegan>.
- Ploner A (2011) *Heatplus: Heatmaps with row and/or column covariates and colored clusters*. R package version 2.1.0. R Foundation for Statistical Computing, Vienna, Austria. Available at: <http://www.bioconductor.org/packages/2.10/bioc/html/Heatplus.html>.
- R Development Core Team (2008) *R: A language and environment for statistical computing*. R Foundation for Statistical Computing, Vienna, Austria. Available at: <http://cran.r-project.org/>.
- Rees G, Baldwin D, Watson G, Perryman S & Nielsen D (2004) Ordination and significance testing of microbial community composition derived from terminal restriction fragment length polymorphisms: application of multivariate statistics. *Antonie Van Leeuwenhoek* **86**: 339–347.
- Rittmann BE (2010) Environmental biotechnology in water and wastewater treatment. *J Environ Eng* **136**: 348–353.
- Robert P & Escoufier Y (1976) A unifying tool for linear multivariate statistical methods: the RV-coefficient. *Appl Statist* **25**: 257–265.
- Schuler AJ & Jenkins D (2003) Enhanced biological phosphorus removal from wastewater by biomass with different phosphorus contents, part I: experimental results and comparison with metabolic models. *Water Environ Res* **75**: 485–498.
- Slater FR, Johnson CR, Blackall LL, Beiko RG & Bond PL (2010) Monitoring associations between clade-level variation, overall community structure and ecosystem function in enhanced biological phosphorus removal (EBPR) systems using terminal-restriction fragment length polymorphism (T-RFLP). *Water Res* **44**: 4908–4923.
- Sun Y, Wolcott RD & Dowd SE (2011) Tag-encoded FLX amplicon pyrosequencing for the elucidation of microbial and functional gene diversity in any environment. *Methods Mol Biol* **733**: 129–141.
- Thierry S, Macarie H, Iizuka T *et al.* (2004) *Pseudoxanthomonas mexicana* sp. nov. and *Pseudoxanthomonas japonensis* sp. nov., isolated from diverse environments, and emended descriptions of the genus *Pseudoxanthomonas* Finkmann *et al.* 2000 and of its type species. *Int J Syst Evol Microbiol* **54**: 2245–2255.
- Urakami T, Araki H, Oyanagi H, Suzuki K-I & Komagata K (1992) Transfer of *Pseudomonas aminovorans* (den Dooren de Jong 1926) to *Aminobacter* gen. nov. as *Aminobacter aminovorans* comb. nov. and description of *Aminobacter aganoensis* sp. nov. and *Aminobacter niigataensis* sp. nov. *Int J Syst Bacteriol* **42**: 84–92.
- Vanwonterghem I, Jensen PD, Ho DP, Batstone DJ & Tyson GW (2014) Linking microbial community structure, interactions and function in anaerobic digesters using new molecular techniques. *Curr Opin Biotechnol* **27**: 55–64.
- Verstraete W, Wittebolle L, Heylen K, Vanparrys B, de Vos P, van de Wiele T & Boon N (2007) Microbial Resource Management: the road to go for environmental biotechnology. *Eng Life Sci* **7**: 117–126.
- Vogelaar JCT, Klapwijk A, van Lier JB & Rulkens WH (2000) Temperature effects on the oxygen transfer rate between 20 and 55 °C. *Water Res* **34**: 1037–1041.
- Volcke EIP, Picioreanu C, De Baets B & van Loosdrecht MCM (2012) The granule size distribution in an anammox-based granular sludge reactor affects the conversion – Implications for modeling. *Biotechnol Bioeng* **109**: 1629–1636.
- Wang X, Hu M, Xia Y, Wen X & Ding K (2012) Pyrosequencing analysis of bacterial diversity in 14 wastewater treatment systems in China. *Appl Environ Microbiol* **78**: 7042–7047.
- Weissbrodt DG, Lochmatter S, Ebrahimi S, Rossi P, Maillard J & Holliger C (2012a) Bacterial selection during the formation of early-stage aerobic granules in wastewater treatment systems operated under wash-out dynamics. *Front Microbiol* **3**: 332.
- Weissbrodt DG, Shani N, Sinclair L, Lefebvre G, Rossi P, Maillard J, Rougemont J & Holliger C (2012b) PyroTRF-ID: a novel bioinformatics methodology for the affiliation of terminal-restriction fragments using 16S rRNA gene pyrosequencing data. *BMC Microbiol* **12**: 306.
- Weissbrodt DG, Neu TR, Kuhlicke U, Rappaz Y & Holliger C (2013a) Assessment of bacterial and structural dynamics in aerobic granular biofilms. *Front Microbiol* **4**: 175.
- Weissbrodt DG, Schneiter GS, Furbinger JM & Holliger C (2013b) Identification of trigger factors selecting for polyphosphate- and glycogen-accumulating organisms in aerobic granular sludge sequencing batch reactors. *Water Res* **47**: 7006–7018.
- Wild HE Jr, Sawyer CN & McMahon TC (1971) Factors affecting nitrification kinetics. *J Water Pollut Control Fed* **43**: 1845–1854.

- Winkler MKH, Bassin JP, Kleerebezem R, de Bruin LMM, van den Brand TPH & van Loosdrecht MCM (2011) Selective sludge removal in a segregated aerobic granular biomass system as a strategy to control PAO-GAO competition at high temperatures. *Water Res* **45**: 3291–3299.
- Yilmaz G, Lemaire R, Keller J & Yuan Z (2008) Simultaneous nitrification, denitrification, and phosphorus removal from nutrient-rich industrial wastewater using granular sludge. *Biotechnol Bioeng* **100**: 529–541.
- Yu CP, Roh H & Chu KH (2007) 17beta-estradiol-degrading bacteria isolated from activated sludge. *Environ Sci Technol* **41**: 486–492.
- Yuan Z & VanBriesen J (2008) Bacterial growth yields on EDTA, NTA, and their biodegradation intermediates. *Biodegradation* **19**: 41–52.

Supporting Information

Additional Supporting Information may be found in the online version of this article:

Fig. S1. Box plot representations of variations in operation, BNR, and microbiological parameters.

Fig. S2. Hierarchical clustering analyses of operation, BNR, and bacterial community data sets of SBR-1 and SBR-2.

Fig. S3. Multiple factor analysis (MFA) providing a picture of the relationships among operation, BNR, and bacterial community data sets of SBR-1.

Table S1. Characteristics and system analysis of SBR-1 and SBR-2.

Table S2. Closest phylogenetic affiliations of OTUs identified from SBR-1 and SBR-2 with PyroTRF-ID.

Table S3. Correlation coefficients used to quantify the relations between operation variables and BNR performances in SBR-1 and SBR-2.

Table S4. Correlation coefficients used to quantify the relations between process parameters and bacterial community structures in both SBRs.